Simulation of ZnO Enhanced SAW Gas Sensor

Hercules G du Plessis[1] and Willem J Perold[1*]
[1]Superconducting, Advanced Materials and Nano Devices Laboratory, Department of Electrical and Electronic Engineering, Stellenbosch University, Stellenbosch, 7600, South Africa

*Corresponding author: Prof. Willem Perold, Department of Electrical and Electronic Engineering, Stellenbosch University, Stellenbosch, 7600, South Africa, wjperold@sun.ac.za

Abstract: Surface acoustic wave (SAW) devices are widely used for their sensing capabilities and gas sensing is only one of the many uses. There is an ever increasing need to make them as effective as possible by adding nanomaterials to the device. In this study a two-port delay-line structure on top of 128YX lithium niobate was simulated with COMSOL Multiphysics in the form of a 2D cross-section. ZnO nanopillars were added to the sensing area of the device to increase sensitivity. Frequency and time dependant simulations were conducted on the device. It was found that even with the ZnO nanopillars the predetermined operating frequency for the SAW device is unchanged. The optimal height for the electrodes of the IDTs was determined to be 200nm.

Keywords: COMSOL, Gas sensor, Lithium niobate, MEMS, Piezoelectric, SAW, Zinc oxide

1. Introduction

Sensors are part of our everyday life and have applications in a variety of fields. These applications include, but are not limited to, diagnostics in the medical field and safety precautions for hazardous gas detection in the industrial field. Nanotechnology is being used increasingly, because of the advantages it brings in efficiency, robustness and cost effectiveness [1].

Micro-electro-mechanical systems (MEMS) are one of the areas that are being used widely for gas sensing purposes and are sometimes in the form of surface acoustic wave (SAW) devices. These devices make use of the piezoelectric effect found in some crystals and ceramics, such as lithium niobate and quartz, to allow an acoustic wave to propagate along the surface of the substrate. Interdigital transducers (IDT) are placed on top of the substrate to transmit and receive the acoustic waves. When an alternating electrical signal is applied to the input, the IDT will convert the electrical energy into mechanical energy. This will be in the form of an acoustic wave. The wave can then be converted back to an electrical signal by placing another IDT in the wave's propagation path. Any perturbation of the wave between the IDTs can be measured in the form of wave attenuation, delay in propagation, characteristic changes, and insertion loss. This setup is commonly referred to as a two-port delay-line configuration. It is best suited for gas sensing and is used as such in this study.

To further increase the sensitivity of sensors, different nanomaterials can be incorporated. This can be done by adding nanostructures or thin films to the detection area between the IDTs. Adding such materials to the propagation path will drastically affect the characteristics of the device in its passive form. This should be investigated to determine the advantages of the nanomaterial and the total affect it has on the SAW device. An optimised sensor for gas detection is a sensor that can detect a hazardous gas well below the concentration that will cause harmful effects.

Previous studies in the field have successfully shown that these SAW sensors can be used in a number of ways. Roa *et al.* [2] used a gold thin film with gold nanostructures to demonstrate that the addition of such structures in the sensing area does indeed have an effect on the wave propagation characteristics and increase sensor performance. Similarly, other studies have been done that shows promising results by using zinc oxide (ZnO) thin films, carbon nanotubes, and aluminium nitride [3-6].

This study will focus on the simulation of ZnO nanopillars on the sensing area of a SAW device, using COMSOL Multiphysics.

2. Theory and materials

In a piezoelectric material the propagation of the acoustic waves are governed by [7]

$$T_{ij} = c^E_{ijkl} S_{kl} - e_{ijk} E_k \qquad (1)$$

$$D_i = e_{ikl} S_{kl} + \varepsilon^S_{ik} E_k \qquad (2)$$

where T represents the stress tensor, c^E the elasticity matrix, S the strain tensor, e the piezoelectric coupling constants, E_k the electric field intensity, and ε^S_{ik} the permeability.

For an optimised SAW device the substrate ideally will have a large electromechanical coupling coefficient (k^2) and SAW wave velocity. Shibayama *et al.* [8] has shown that 128YX lithium niobate has a high k^2 coefficient and velocity, as well as giving much less excitation of unwanted bulk waves. For an anisotropic piezoelectric material such as lithium niobate the material constants have the following form and values, as seen in equations (3-5) and Table 1 [9].

$$c = \begin{pmatrix} c_{11} & c_{12} & c_{13} & c_{14} & 0 & 0 \\ c_{12} & c_{11} & c_{13} & -c_{14} & 0 & 0 \\ c_{13} & c_{13} & c_{33} & 0 & 0 & 0 \\ c_{14} & -c_{14} & 0 & c_{44} & 0 & 0 \\ 0 & 0 & 0 & 0 & c_{44} & c_{14} \\ 0 & 0 & 0 & 0 & c_{14} & (c_{11} - c_{12})/2 \end{pmatrix} \qquad (3)$$

$$e = \begin{pmatrix} 0 & 0 & 0 & 0 & e_{15} & -e_{22} \\ -e_{22} & e_{22} & 0 & e_{15} & 0 & 0 \\ e_{31} & e_{31} & e_{33} & 0 & 0 & 0 \end{pmatrix} \qquad (4)$$

$$\varepsilon = \begin{pmatrix} \varepsilon_{11} & 0 & 0 \\ 0 & \varepsilon_{11} & 0 \\ 0 & 0 & \varepsilon_{33} \end{pmatrix} \qquad (5)$$

Table 1. Material constants used for 128YX lithium niobate

Elastic constants	c_{11}	2.03 x 10^{11} N/m^2
	c_{12}	0.573
	c_{13}	0.752
	c_{14}	0.085
	c_{33}	2.424
	c_{44}	0.595
Piezoelectric coupling constants	e_{15}	3.7 C/ m^2
	e_{22}	2.5
	e_{31}	0.23
	e_{33}	1.33
Permeability constants	ε_{11}	85.2
	ε_{33}	28.7
Density	ρ	4700 kg / m^3

ZnO has successfully been used in a variety of gas sensor studies in the form of a thin film, but less so in the form of nanopillars. Bie *et al.* [10] showed that ZnO holds a lot of potential to develop stable and sensitive gas sensors. ZnO is one of COMSOL Multiphysics' built-in materials, thus the piezoelectric and mechanical properties for ZnO were taken from there.

In a two-port delay-line configuration the dimensions of the IDT determines the wavelength of the acoustic wave. In the equation

$$\lambda = 2(W_e + W_{sp}) \qquad (6)$$

the wavelength, λ, is determined by the width of each electrode, W_e, and the space between each electrode, W_{sp}. The operating frequency is governed by

$$f_0 = \frac{v_0}{\lambda} \qquad (7)$$

where v_0 is the propagation velocity of the acoustic wave in the piezoelectric material [10].

3. Use of COMSOL Multiphysics

To keep simulation time and hardware requirements of the simulation bearable a 2D model of a cross-section of the SAW device was created. The sensor was designed to work with a wavelength of 80µm. The operating frequency is then calculated to be 46.9 MHz. The lithium niobate substrate was created with dimensions of 520µm by 200µm. On top of the substrate the two IDTs were placed with a height of 200nm and electrode width of 20µm, consisting of aluminium. According to the wavelength design choice each electrode had to be spaced 20µm from each other. Each IDT has two pairs of electrodes and the distance between the input and output IDT is a single wavelength. At either side of the sensor three reflectors were placed, with a width and spacing of 10µm each. Finally, a block of air, to compensate for the atmosphere, and with a height of 10µm, was placed on top of the substrate with the IDTs and reflectors incorporated inside.

The ZnO nanopillars are added to the centre of the detection area. Because of the 2D simplification, the cylindrical nanopillars were also simplified to rectangular shapes with width of 50nm. The height of the nanopillars were chosen to be 200nm as this was determined to be in the region of the optimal height for nanopillars as discussed by Zhang [11] and Water *et al.* [12]. The nanopillars were arrange in a simplified array of 60 nanopillars spaced 1µm apart.

Figure 1 shows the meshed cross-section model. The maximum node size was chosen to be smaller than a fifth of the wavelength to ensure that the appropriate harmonics are compensated for. This resulted in 47623 elements in the mesh.

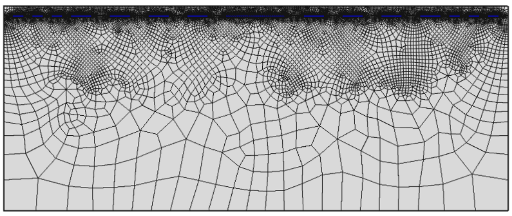

Figure 1 Meshed image of the 2D cross-section of the SAW device with ZnO.

4. Results and discussion

First of all a frequency dependant study was performed. From the results the operating frequency could be determined, as seen in Figure 2. In Figure 3 the acoustic wave can be observed, at the determined operating frequency, traveling at the top of the substrate.

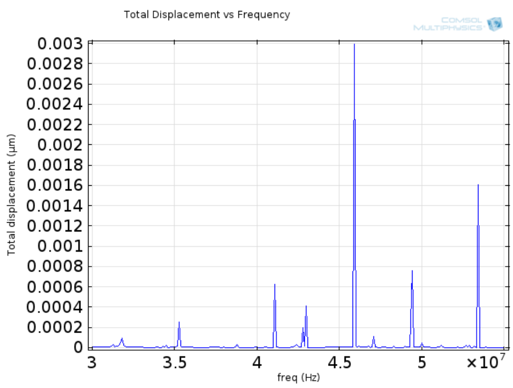

Figure 2 Frequency sweep showing maximum displacement at center frequency.

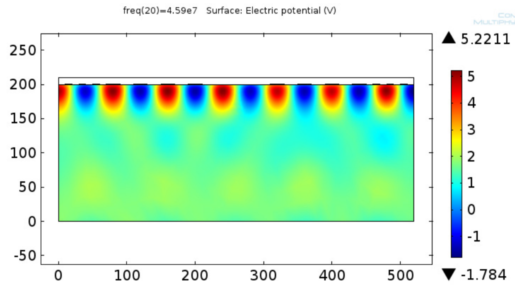

Figure 3 2D image of the acoustic wave at the operating frequency.

Next a parameter sweep of the electrode height was done during the frequency dependant study. This was done by first sweeping the parameter from 200nm to 800nm at a step size of 100nm, as seen in Figure 4. A more precise sweep was done afterwards from 100nm to 300nm at a step size of 10nm. The optimal height for the electrodes of the transducers was found to be 200nm.

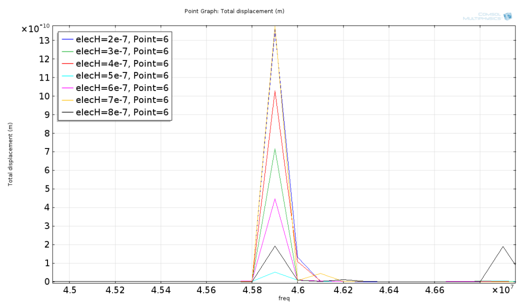

Figure 4 Displacement of the substrate for the parameter sweep of the eltrode height.

7. Conclusion

A simulation of a SAW device was performed to investigate how added ZnO nanopillars in the sensing area affect the SAW device's properties. The nanopillars did not have an effect on the theoretical calculated operating frequency of the device. With the nanopillars on the substrate it was determined that the optimal electrode height for the IDTs was 200nm. Future work includes the optimal height of the ZnO nanopillars as well as the simulation of the full sensor inside a hazardous gaseous environment.

8. References

1. Morgan, David P, History of SAW devices, *IEEE International Frequency Control Symposium,* 439-460 (1998)

2. Rao, Yeswanth L and Zhang, Guigen, 3-D finite element modeling of nanostructure enhanced SAW sensor, *Proc. COMSOL Users Conf* (2006)

3. Ahmadi, S and Hassani, F and Korman, C and Rahaman, M and Zaghloul, M, *Characterization of multi-and single-layer structure SAW sensor*, Sensors, 2004. Proceedings of IEEE, 1129-1132, IEEE (2004)

4. Penza, M and Aversa, P and Cassano, G and Wlodarski, W and Kalantar-Zadeh, K, Layered SAW gas sensor with single-walled carbon nanotube-based nanocomposite coating, *Sensors and actuators B: Chemical*, **127**, 168-178 (2007)

5. Di Francia, Girolamo and Alfano, Brigida and La Ferrara, Vera, Conductometric gas nanosensors, *Journal of Sensors*, **2009** (2009)

6. Atashbar, MZ and Sadek, AZ and Wlodarski, W and Sriram, S and Bhaskaran, M and Cheng, CJ and Kaner, RB and Kalantar-Zadeh, K, Layered SAW gas sensor based on CSA synthesized polyaniline nanofiber on AlN on 64° YX $LiNbO_3$ for H_2 sensing, *Sensors and Actuators B: Chemical*, **138**, 85-89 (2009)

7. Meitzler, A and Tiersten, HF and Warner, AW and Berlincourt, D and Couqin, GA and Welsh III, FS, IEEE standard on piezoelectricity, 1988

8. Shibayama, KIMIO and Yamanouchi, KAZUHIKO and Sato, HIROAKI and Meguro, TOSHIYASU, Optimum cut for rotated Y-cut $LiNbO_3$ crystal used as the substrate of acoustic-surface-wave filters, *Proceedings of the IEEE*, **64**, 595-597 (1967)

9. Yang, Jiashi, *Analysis of piezoelectric devices*, World Scientific Singapore (2006)

10. Bie, Li-Jian and Yan, Xiao-Na and Yin, Jing and Duan, Yue-Qin and Yuan, Zhi-Hao, Nanopillar ZnO gas sensor for hydrogen and ethanol, *Sensors and Actuators B: Chemical*, **126**, 604-608 (2007)

11. Zhang, Guigen, Nanostructure-enhanced surface acoustic waves biosensor and its computational modeling, *Journal of Sensors*, **2009** (2009)

12. Water, Walter and Chen, Shih-En, Using ZnO nanorods to enhance sensitivity of liquid sensor, *Sensors and Actuators B: Chemical*, **136**, 371-375 (2009)

8. Author, Article title, *Journal*, **Volume**, page numbers (year)
9. Author, *Book title*, page numbers. Publisher, place (year)